Demand Response Power-Gas Interconnection Energy System and Power Metering Based on SOGA

QianQian Cai[1], Xiao Jiang[1], ZheHeng Liang[2], ShiMeng Du[3] and ShiFeng Jiang[4,*]

[1]*Metrology Center of Guangdong Power Grid Corporation, Guangzhou, 510062, Guangdong, China*
[2]*Information Center of Guangdong Power Grid Co., Ltd., Guangzhou, 510180, Guangdong, China*
[3]*Guangdong power grid limited liability company Yunfu power supply bureau, Yunfu, 527300, Guangdong, China*
[4]*Guangzhou Luoli Energy Technology Co., Ltd, Guangdong, 510000, Guangdong, China*
E-mail: luoliny2020@163.com
[*]*Corresponding Author*

Received 24 December 2023; Accepted 22 January 2024

Abstract

Under the double background of global energy crisis and environmental pollution, China vigorously develops renewable energy while accelerating the construction of energy Internet. Taking demand response into account, this paper proposes the optimal design of power-gas interconnection energy system and power metering, and establishes the optimization research model of IEGES (integrated electricity-gas energy system) with demand response. Firstly, the structure model of the electric-gas interconnection energy system with CHP (Cogeneration, combined heat and power) as the core is constructed, and the energy conversion relationship and different energy flow

Strategic Planning for Energy and the Environment, Vol. 43_3, 685–714.
doi: 10.13052/spee1048-5236.4339

directions of the coupling equipment are expounded from three aspects. The natural gas source point, pipeline equation, power side branch equation, voltage and current equation are modeled and sorted out, and the square term in the equation is linearized by second-order cone programming method, and the mixed integer nonlinear programming problem is transformed into mixed integer linear programming problem. A single objective genetic algorithm with "elite strategy" was selected to solve the equipment capacity optimization problem of IEGES system with system economy as the optimization objective. After a long time of parameter combination attempts, the current population size is 30, the number of iterations is 600, the crossover rate is 0.8, and the heritability is 0.3. The above parameters can obtain better convergence results on the basis of considering the operation time. Finally, a stochastic optimization method of energy Internet considering integrated demand response and uncertainty of wind power is proposed, which aims to meet the energy demand of end users while minimizing the operating cost of the system. The comprehensive demand response strategy including internal and external demand response is considered in the model. Internal demand response is realized by adjusting the internal operation mode of EH, while external demand response is implemented by the end user's active response, and the load is time-shifted or interrupted under the guidance of external signals.

Keywords: Demand response, power-gas interconnection energy system, CHP, single objective genetic algorithm, electric power measurement.

1 Introduction

The rapid development of the national economy has improved the quality of life of the people, but also brought serious energy depletion and environmental pollution crisis. On the one hand, the non-renewable primary energy requires accelerating the development of new energy and improving energy utilization efficiency. On the other hand, the traditional energy system of independent management of all types of energy has limited the improvement of comprehensive energy utilization efficiency. With the nonstop improvement and maturity of science and technological know-how and Internet technology, as well as the improvement and enchantment of cloud computing, massive statistics Internet of Things, Genius, and blockchain technology, the thinking of electricity Internet got here into being [1]. Energy Internet is a new kind of strength utilization gadget fashioned via integrating

the traits of superior records science and new electricity technology. It uses power electronics technology, information technology, and intelligent control technology to closely connect distributed energy and energy load nodes, and promote the interconnection and flow of energy and mutual exchange of shared networks [2]. The organization and construction of an integrated energy system is an important landing development project to achieve the strategic goal of the energy Internet. With the increasingly severe energy challenges, under the background of green and low-carbon, the advantages and roles of integrated energy systems in solving the above problems are becoming increasingly obvious.

At present, He Yufei et al. proposed an emergency resource pre-disaster cooperative scheduling strategy based on a typical power-gas interconnection energy system [3]. Qiu Gefei et al., aiming at the hassle of non-economic operation of power-gas interconnection built-in power gadget prompted by way of the uncertainty of supply and load, constructed a fuzzy most efficient scheduling mannequin of power-gas interconnection built-in strength device of industrial park thinking about the uncertainty of supply and load [4]. Li Jinghua et al. focused on measuring the energy supply reliability of IEGES and improved the "electric-oriented" IEGES transmission network planning model [5]. Wei Zhenbo et al. proposed a multi-objective prolonged planning mannequin for a built-in power-gas interconnection strength machine based totally on the data hole choice principle [6].

Taking demand response into account, this paper proposes the optimal design of a power-gas interconnection energy system and power metering and establishes the optimization research model of IEGES with demand response. Firstly, the structure model of the electric-gas interconnection energy system with CHP as the core is constructed, and the energy conversion relationship and different energy flow directions of coupling equipment are expounded from three aspects: energy input, energy combination, and energy consumption. Then, the power side price demand response model is considered comprehensively. The herbal fuel supply point, pipeline equation, energy facet department equation, voltage, and present-day equation are modeled, and the rectangular period in the equation is linearized via the second-order cone programming method, and the combined integer nonlinear programming trouble is modified into a combined integer linear programming problem. A single objective genetic algorithm with "elite strategy" is selected to solve the equipment capacity optimization problem of IEGES system with system economy as the optimization goal, and the genetic algorithm is improved by analyzing the operation characteristics of IEGES system and

changing the number of optimization variables. After a long time of trying to combine the parameters, the current population size is 30, the number of iterations is 600, the crossover rate is 0.8, and the heritability is 0.3. The above parameters can obtain good convergence results on the basis of considering the operation time.

2 Electric-Gas Interconnection Energy System Planning Model

2.1 Energy Structure

The comprehensive energy system can integrate various forms of energy in a certain area, achieve cascade utilization, promote the consumption of renewable energy, and improve the efficiency of energy utilization. Compared with traditional independent power systems, thermal systems, and natural gas systems, IEGES has a more complex composition structure and energy coupling relationship, and the equipment differences among energy units are more significant [7]. Generally speaking, IEGES contains both electrical energy, which is not easy to store in large quantities, and thermal energy and cold energy, which are easy to store and have large inertia. The energy unit includes both component-level devices and combined devices (such as CHP, and CCHP systems). As a basis for the study of energy coupling and transformation in an integrated energy system, the integrated power-gas power flow is of great value [8]. In this chapter, the model of power-gas integrated power flow is analyzed from three perspectives: source, net, and load. Source-side models include probabilistic output models for distributed wind and PV, as well as energy-coupled devices (e.g. CHP, GB) models in the system. The community mannequin consists of an electricity system, thermal machine, and herbal fuel device model. The demand response mannequin of interruptible electrical and thermal load is analyzed. The shape sketch is proven in Figure 1.

In addition, as can be seen from Figure 1, IEGES constructed in this paper mainly includes energy flow and IDR information flow:

(1) Energy flow. IES covers cold, heat, electricity, and gas loads. The electrical energy load is furnished with the aid of CHP units, photovoltaics, and the strength grid, and extra electrical energy can be brought to the higher electricity grid [9]. The cooling load is furnished with the aid of absorption chillers and electric-powered chillers. The warmness load is at the same time furnished using CHP, gasoline boiler,

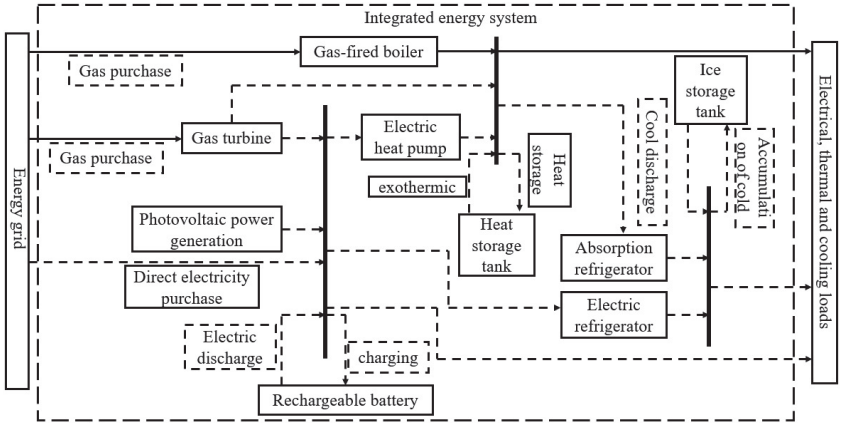

Figure 1 Energy system structure diagram.

and electric-powered pushed warmness pump, and the warmth storage gadget can be considered as the warmth load when storing strength and the warmness supply when releasing warmness energy. The gas load is supplied directly by natural gas.

(2) IDR. Implement a price-based IDR in an integrated energy system, and the user changes the way he uses energy according to the price signal. Some of the cold, hot, and electrical loads are directly reduced, transferred, or converted between the three, and are supplied by coupling devices [10]. The other part is converted to the gas load, which is directly supplied by natural gas.

2.2 Model of Unit Equipment in Power-Gas Interconnection Energy System

Based on the concept of cascade utilization of energy, CHP units use high-grade energy (clean natural gas) to generate electricity and recycle low-grade energy (waste heat) generated by the prime mover for heating and providing domestic hot water, etc., realizing the reuse of power generation waste heat.

Gas turbines and waste heat recovery units are the two-core equipment in CHP [11]. The basic principle of CHP operation is as follows: The gas turbine uses a mixture of natural gas and air as fuel to produce high-temperature and high-pressure gas, which drives the generator to run and generate electric energy. The high-temperature smoke generated by combustion is collected into the waste heat recovery device, and hot water or high-temperature steam

is produced after treatment, which is used for heating or other projects [12]. The micro gas turbine is the most commonly used engine in CHP because of its small size, high working efficiency, and fast starting speed. The energy utilization rate of CHP units with micro gas turbine as the core can reach 70%∼90%. The physical model of CHP includes two parts: electricity and heat production, which can be expressed as:

$$P'_{GT} = P'_{CHP} \cdot \eta_{GT} = \frac{V^t_{gCHP} \cdot \beta \cdot \eta_{GT}}{\Delta t} \tag{1}$$

$$H^t_{HE} = P'_{CHP} \cdot \eta_{HE} \tag{2}$$

Similar to the standard strength gadget strength drift calculation model, the strength device mannequin of the built-in electricity gadget nonetheless adopts the classical AC energy glide mannequin in the built-in electricity waft calculation, and the node energy expression is as follows:

$$\begin{cases} P_i = v_i \sum\limits_{j \in i} v_j (G_{ij} \cos\theta_{ij} + B_{ij} \sin\theta_{ij}) \\ Q_i = v_i \sum\limits_{j \in i} v_j (G_{ij} \sin\theta_{ij} + B_{ij} \cos\theta_{ij}) \end{cases} \tag{3}$$

P_i and Q_i are respectively the injected active power and reactive power of node i in the power grid. v_i and v_j are the voltage amplitudes of nodes i and j.

Different from electromagnetic propagation, natural air flow in gas transmission networks has the characteristics of long delay and large inertia. By analogy with the modeling method of a power system, the physical quantity in the natural gas system can be simplified into two types: branch quantity and node quantity. A natural gas system can be characterized by branch state quantity, node state quantity, and topological constraint relationship satisfied by branch node [13]. The relationship between node strain and pipeline waft in the herbal gasoline community is described as follows:

$$\Psi_{ij} = \begin{cases} W_{ij}\sqrt{(p_i^2 - p_j^2)} & p_i < p_j \\ -W_{ij}\sqrt{(p_j^2 - p_i^2)} & p_j < p_i \end{cases} \tag{4}$$

Where: Ψ_{ij} represents the gas flow from node i to node j. W_{ij} represents the Weymouth equation constant in the ij section of a natural gas pipeline. P_i represents the absolute gas pressure at node i.

The flow continuity equation of the natural gas network can be described by Equation (5):

$$A_g \Psi = \Psi_q \tag{5}$$

Where: A_g is the node-branch association matrix of the natural gas network. Ψ is the flow rate of natural gas in each pipeline. Ψ_q indicates the outgoing traffic of each node.

Absorption chillers can without delay use low-grade thermal electricity such as boiler steam, waste heat, or even waste warmth as the riding supply for refrigeration, realizing cascade utilization of energy, enhancing electricity utilization effectivity, and decreasing waste warmness air pollution [14]. Absorption chillers can be divided into ammonia absorption chillers and lithium bromide absorption chillers according to the different refrigerants and absorbers. Ammonia water refrigerators with ammonia water solution as refrigerant and absorbent, are mainly used in refrigeration and chemical industry production, but this type of equipment metal consumption is large, and ammonia is corrosive to metal, is no longer promoted. The lithium bromide unit uses water as refrigerant and lithium bromide as absorbent, which has stable chemical properties, better refrigeration performance, and good utilization of waste heat and waste heat [15]. Therefore, this paper adopts the lithium bromide absorption chiller as one of the cold source equipment in IEGES. The specific physical model is as follows:

$$CO'_{AC} = \eta_{AC} \cdot H^t_{AC} \tag{6}$$

Where CO'_{AC} represents the cold power output of the absorption refrigerator at time t H'_{AC} represents the thermal power input to the absorption chiller at the moment.

An electric refrigerating machine is a kind of electric-cold coupling equipment, that uses a compression device to liquefy refrigeration gas, and then uses the principle of evaporation and heat absorption of liquefied refrigerant to convert electric energy into cold energy. According to the different compressors, electric chillers can be divided into screw chillers and scroll chillers. Compared with absorption chillers, it uses high-grade electrical energy, so the cooling efficiency is higher and the reliability is higher.

When IDR is taken into account, the output of electric chillers and absorption chillers can be optimized according to the level of electricity price, and the output of electric chillers is usually increased when the electricity price is low or the waste heat is insufficient [16]. At peak load, the electric refrigerator can also be used as an auxiliary unit of the absorption refrigerator to supplement the insufficient cooling energy supplied by the absorption refrigerator.

The physical model of the electric refrigerator can be expressed as:

$$CO_{EC}^{t} = \eta_{EC} \cdot P_{EC}^{t} \tag{7}$$

In an integrated energy system, CHP units always produce both electrical and thermal energy at the same time according to a certain thermoelectric ratio, but the actual thermal (cold) load and electrical load often do not match. After adding the heat storage device, the thermoelectric decoupling can be realized to some extent, and the mismatch between the actual load thermoelectric ratio and the thermoelectric ratio of the CHP unit can be reduced. When the demand for electrical load is high and the demand for hot (cold) load is low, heat storage tanks can be used to store heat to reduce heat waste. On the contrary, when the demand for electrical load is low and the demand for hot (cold) load is high, a part of the heat can be provided by the heat storage tank to improve the economy of the system operation. The model of the heat storage tank can be expressed as:

$$Q_{HS}^{t+1} = (1 - \mu_{Loss})Q'_{HS} + \left(H'_{ch} \cdot \eta_{ch} - \frac{H_{dch}^{t}}{\eta_{dch}}\right) \cdot \Delta t \tag{8}$$

2.3 Coupled Device Model

Natural gas combustion heats water to produce a large amount of high-temperature steam, sends high-grade heat into GT, drives the blade to rotate to drive the generator to generate electricity, and sends medium/low-grade heat into the waste heat boiler, which is collected for heating and domestic hot water supply. Among them, the operating efficiency of GT is related to its load rate and the operating characteristic model is shown as follows:

$$\eta_{E}^{GT} = (0.8264 \cdot PLR^{3} - 2.334 \cdot PLR^{2} + 2.329 \cdot PLR + 0.1797)\eta_{\mathrm{nom\_E}}^{GT} \tag{9}$$

$$c_m = \frac{\eta_{H}^{GT}}{\eta_{E}^{GT}} \tag{10}$$

$$\Phi_{GT} = P_{\mathrm{GT}} c_m \eta_r \tag{11}$$

$$\eta_{g-e}^{\mathrm{CHP}} = \frac{P_{GT}}{\Psi_{\mathrm{GT}}} \tag{12}$$

As society has increasingly higher requirements on the safety, economy, and environmental protection of the energy system, GB has become the preferred equipment in the heat production industry due to a series of significant

advantages such as small size, flexible layout, less pollutant emission, high efficiency, safety, and reliability, and has been widely used in the heating and hot water supply of factories, enterprises, and northern cities [17]. At present, GB is one of the most commonly used heat source equipment, and its output thermal power is related to the amount of fuel consumed, considering the efficiency relationship between the output heat and the amount of input fuel to describe the mathematical model of gas boiler:

$$\eta_{\varepsilon} = \frac{\Phi_{t,\mathrm{GB}}}{F_{t,\mathrm{GB}}} \tag{13}$$

$$F_{t,\mathrm{GB}} = V_{t,GB} LHV_{NG} \tag{14}$$

The fan output probability model is mainly related to the wind speed probability model and the fan output characteristics. At present, the commonly used probability models for fitting wind speed include normal distribution, Weibull distribution, Log-logistic distribution, etc. In this paper, Weibull distribution, which is the most widely used, is selected, as shown in Equation (15):

$$f(v) = \frac{k}{c}\left(\frac{v}{c}\right)^{k-1} e^{-\left(\frac{v}{c}\right)^{k}} \tag{15}$$

When the wind speed is *v*, the output power $P_{wd}(v)$ of the fan is shown in (16).

$$P_{wd}(v) = \begin{cases} 0, & v < v_{ci}, v > v_{co} \\ k_1 v + k_2, & v_{ci} < v \le v_N \\ P_{wd,N}, & v_N < v \le v_{co} \end{cases} \tag{16}$$

Bring Equation (16) into (15) to get the fan output probability model, as shown in Equation (17).

$$f(P_{wd}) = \begin{cases} 1 - \exp\left[-\left(\dfrac{v_{ci}}{c}\right)^{k}\right] + \exp\left[-\left(\dfrac{v_{co}}{c}\right)^{k}\right], & P_{wd} = 0 \\ \dfrac{k}{k_1 c}\left(\dfrac{P_{wd} - k_2}{k_1 c}\right)^{k-1} \exp\left[-\left(\dfrac{P_{wd} - k_2}{k_1 c}\right)^{k}\right], & 0 < P_{wd} \le P_{wd,N} \\ \exp\left[-\left(\dfrac{v_N}{c}\right)^{k}\right] - \exp\left[-\left(\dfrac{v_{co}}{c}\right)^{k}\right], & P_{wd} = P_{wd,N} \end{cases} \tag{17}$$

The output probability model of photovoltaic is mainly derived from the probability model of light intensity and the relationship model between photovoltaic power generation and light intensity. The probability distribution model of light intensity is usually expressed by the Beta model, as shown in Equation (18):

$$f(r) = \frac{\Gamma(\alpha+\beta)}{\Gamma(\alpha)\Gamma(\beta)} \left(\frac{r}{r_{\max}}\right)^{\alpha-1} \left(1-\frac{r}{r_{\max}}\right)^{\beta-1} \tag{18}$$

Under a certain temperature condition, the electric power output of photovoltaics is approximately proportional to the light intensity, so the probability model of photovoltaic output is derived as shown in Equation (19).

$$f(r) = \frac{\Gamma(\alpha+\beta)}{\Gamma(\alpha)\Gamma(\beta)} \left(\frac{P_{pv}}{P_{pv,\max}}\right)^{\alpha-1} \left(1-\frac{P_{pv}}{P_{pv,\max}}\right)^{\beta-1} \tag{19}$$

3 IEGES Decoupling Cooperative Scheduling Under Demand Response

3.1 Optimization Model of Energy System Taking Demand Side Into Account

Compared with the traditional power demand response, the demand side response behavior of the integrated energy system changes from the horizontal time and is updated to the combination of the vertical energy type transformation and the horizontal time transfer. At the same time, based on traditional power demand response, users' demand for heterogeneous energy such as cold, heat, and electricity is included in the category of demand-side resources [18]. Integrated demand response is a broader interaction relationship between various energy sources and energy prices, using research advances in various sciences, energy technologies in the context of energy Internet. Considering the terminal load demand, stimulate load flexibility, improve the coupling between a variety of heterogeneous energy sources, strengthen the in-depth coordination of source, network, load and storage, improve the utilization efficiency of renewable energy, and reduce the energy consumption cost on the user side. In addition, it offers enough propulsion for consumers to behave in the appropriate ways. Figure 2 depicts the conceptual design of a demand-side integrated energy system.

Research on the operation optimization approach of demand-side built-in electricity devices can enhance the effectivity of demand-side strength

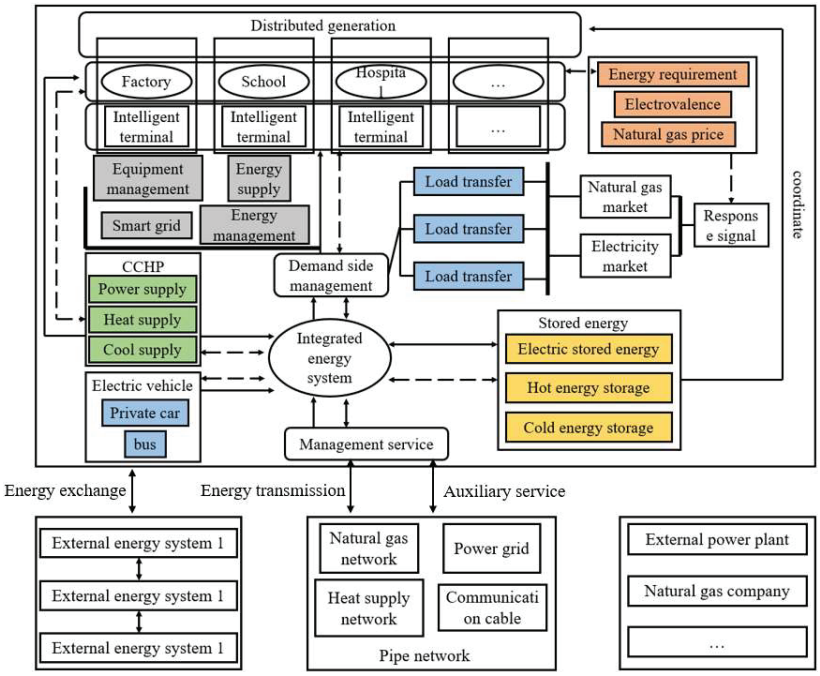

Figure 2 Schematic diagram of the demand-side energy system.

utilization, and rational allocation of sources, and amplify the gain of electricity saving and emission reduction. It is of top-notch importance to promote the development of China's new electricity gadget with new electricity as the most important body, promote the method of electricity revolution, assist in understanding the dual-carbon goal, and assist the improvement of the countrywide electricity economic system [19]. Compared with ordinary strength demand response, the essential benefits of demand response in built-in strength structures are as follows.

(1) Improving economy. With the implementation of demand-side response, the diploma of electricity coupling inside the built-in electricity gadget is getting greater and higher, and the diploma of horizontal and vertical coordination and optimization is getting greater and higher, which improves the integration stage of the complete built-in strength system and reduces the running fee of the whole machine via gadget integration on the one hand. On the other hand, the consumer actively participates in the demand response, saves the user's strength use cost, improves the financial system of strength use, and as a result can gain greater benefits.

(2) Increase adaptability. The demand-side response can be implemented in the integrated energy system to address the issue of unstable renewable energy output and to increase the flexibility of system regulation, taking into account the intermittent and unpredictable nature of renewable energy as well as the widening peak-valley load gap. At the same time, energy storage's quick growth opens up new demand response application possibilities, and energy storage is a key strategy for boosting the power system's flexibility.

3.2 Demand Response Modeling and Objective Function

With the reform of the electricity market, electric energy also has a certain commodity attribute, according to the economic principle of electricity demand is affected by the price. DR Aims to guide users' electricity consumption behavior through electricity price, and users spontaneously adjust their electricity consumption plan to reduce consumption. Price-based DR Is conducive to optimizing load curves, reducing peak-valley differences, and improving energy optimal allocation [20]. The modeling of price type DR Usually uses the demand price elasticity matrix to describe the impact of electricity price on users, and its expression is as follows.

$$E = \frac{\Delta P}{P_0} \frac{\rho_i}{\Delta \rho} \tag{20}$$

In the real case, the electrical energy rate modifications over time, and the electrical energy demand on the consumer facet is affected by using the electrical energy price. Therefore, there is a positive relationship between electrical energy demand and electrical energy charge on the time scale, that is, the exchange of electrical energy rate in a positive time length will no longer solely have an effect on the load in this period. Moreover, the load of different time intervals will additionally be affected [21]. Therefore, the charge elasticity coefficient of demand response can be divided into two types, one is the self-elasticity coefficient and the other is a cross-elasticity coefficient. Its expression is as follows.

$$E_{ii} = \frac{\Delta P_i}{P_i} \frac{\rho_i}{\Delta \rho_i} \tag{21}$$

$$E_{ij} = \frac{\Delta P_i}{P_i} \frac{\rho_j}{\Delta \rho_j} \tag{22}$$

If a scheduling cycle is divided into 24 periods, the price DR Model can be described as follows.

$$\begin{bmatrix} \dfrac{\Delta P_1}{P_1} \\ \dfrac{\Delta P_2}{P_2} \\ \vdots \\ \dfrac{\Delta P_{24}}{P_{24}} \end{bmatrix} = \begin{bmatrix} E_{1,1} & \cdots & E_{1,24} \\ \vdots & \ddots & \vdots \\ E_{1,1} & \cdots & E_{1,24} \end{bmatrix} \begin{bmatrix} \dfrac{\Delta \rho_1}{\rho_1} \\ \dfrac{\Delta \rho_2}{\rho_2} \\ \vdots \\ \dfrac{\Delta \rho_{24}}{\rho_{24}} \end{bmatrix} \tag{23}$$

Therefore, primarily based on the above analysis, this paper divides the electricity load into residential, industrial, and industrial electrical energy consumption. To facilitate calculation, a unified mathematical mannequin of DR Based on charge is established. The person mechanically adjusts the strength consumption dependency by the sign of rate change, to reap the reason for height slicing and valley filling. The load demand response mannequin of every length after response can be expressed as.

$$\begin{cases} P_{j,t}^{\mathrm{D}} = P_{j,t}^{\mathrm{D,pre}}(1+\alpha) \\ \alpha = \displaystyle\sum_{t=1}^{\mathrm{T}} E_{\mathrm{e},tt'}(\rho_{\mathrm{e},t} - \rho_{\mathrm{e},t}^{\mathrm{pre}})/\rho_{\mathrm{e},t}^{\mathrm{pre}} \end{cases} \tag{24}$$

Considering the actual power situation, the load power of the system needs to be further constrained. It is believed that there is a certain relationship between the reactive load before and after the response and the active load of the system. The model is shown as follows.

$$\begin{cases} P_{j,\min}^{\mathrm{D}} \le P_{j.t}^{\mathrm{D}} \le P_{j,\max}^{\mathrm{D}} \\ Q_{j,t}^{\mathrm{D}} = P_{j.t}^{\mathrm{D}} Q_{j,t}^{\mathrm{D,pre}} / P_{j.t}^{\mathrm{D,pre}} \end{cases} \tag{25}$$

The IEGES optimization scheduling model established in this chapter mainly reflects the premise that the power side and the natural gas side can operate safely and reliably to achieve the optimal system economy. In addition, to replicate the absorption impact of demand response on allotted energy, the goal characteristic of the mannequin is to limit the running cost, and common consideration is given to the energy buy cost, community loss,

wind abandonment value, and mild abandonment cost.

$$\min F_1 = \sum_{t=1}^{T} \left(\sum_{j \in N^{\mathrm{sub}}} c_{\mathrm{sub}} P_{j,t}^{\mathrm{sub}} + \sum_{ij \in N^{\mathrm{Ine}}} c_{1\mathrm{oss}} r_{ij} I_{ij,t}^2 + \sum_{j \in N^{\mathrm{DG}}} c_{\mathrm{DG}} (P_{j,s,t}^{\mathrm{PRE}} - P_{j,s,t}^{\mathrm{DG}}) \right) \tag{26}$$

3.3 Optimization Model Solving Based on SOGA

The decision model is a dynamic reactive power optimization model of a distribution network with continuous and discrete variables, which is non-convex and non-linear and belongs to the NP problem. The power flow equation of the power side branch and the node pressure of the natural gas pipeline in IEGES have square terms. The original model is a MINLP problem, which is difficult to solve with existing commercial solvers [22]. Therefore, the paper will use the SOCP method to transform the square term contained in the model into a first term, to facilitate the solution.

The second-order cone programming can be convocated and relaxed by IEGES, which greatly simplifies the solution. The original complex model can be transformed into the SOCP model which is easy to solve quickly, and complex variables can be represented by a special form cone set. Where the standard form of second-order cone programming is.

$$\begin{cases} \min f(x) \\ s.t.\ Ax = b, x \in K \end{cases} \tag{27}$$

Second order cone:

$$\mathbf{K} = \left\{ x_i \in \mathbf{R^N} |\ y^2 \geq \sum_{i=1}^{n} x_i^2, y \geq 0 \right\} \tag{28}$$

According to the characteristics of the second-order cone, a new linear variable is introduced to replace the original square term for power side branch power flow equation, branch power flow constraint condition, natural gas pipeline node pressure equation and objective function, and the original model in IEGES is transformed into SOCP model.

$$\begin{cases} \tilde{I}_{ij,t} = I_{ij,t}^2 \\ \tilde{V}_{i,t} = V_{i,t}^2 \end{cases} \tag{29}$$

The method of second-order cone programming is used to carry out equivalent deformation in the electric-gas integrated energy system.

$$\begin{cases} \sum\limits_{i\in\alpha(j)}(P_{ij,t}-r_{ij}\tilde{I}_{ij,t})-\sum\limits_{k\in\beta(j)}P_{jk,t}=P_{j,t}^{\mathrm{sub}}+P_{j,t}^{\mathrm{DG}}+P_{j,t}^{\mathrm{GT}}-P_{j,t}^{\mathrm{D}} \\ \sum\limits_{i\in\alpha(j)}(Q_{ij,t}-x_{ij}\tilde{I}_{ij,t})-\sum\limits_{k\in\beta(j)}Q_{jk,t}=Q_{j,t}^{\mathrm{sub}}+Q_{j,t}^{\mathrm{DG}}-Q_{j,t}^{\mathrm{D}} \end{cases} \tag{30}$$

$$\tilde{V}_{j,t}=\tilde{V}_{i,t}-2(r_{ij}P_{ij,t}+x_{ij}Q_{ij,t})+(r_{ij}^2+x_{ij}^2)\tilde{I}_{ij,t} \tag{31}$$

Among them:

$$\tilde{I}_{ij}^t=\frac{(P_{ij}^t)^2+(Q_{ij}^t)^2}{\tilde{V}_i^t} \tag{32}$$

Relax this formula to get:

$$\tilde{I}_{ij}^t\geq\frac{(P_{ij}^t)^2+(Q_{ij}^t)^2}{\tilde{V}_i^t} \tag{33}$$

Then the equivalent deformation is further transformed into the following second-order cone form:

$$\left\|\begin{matrix}2P_{ij.t}\\2Q_{ij,t}\\\tilde{V}_{i,t}-\tilde{I}_{ij,t}\end{matrix}\right\|\leq\tilde{V}_{i,t}+\tilde{I}_{ij,t} \tag{34}$$

The security constraint becomes:

$$\begin{cases} V_{j,\min}^2\leq\tilde{V}_{j.t}\leq V_{j,\max}^2 \\ 0\leq\tilde{I}_{ij,t}\leq I_{ij,\max}^2 \end{cases} \tag{35}$$

Similarly, the corresponding second-order cone form is obtained by optimizing the pressure relaxation of natural gas pipeline nodes:

$$\left\|\begin{matrix}Q_{ij,t}^{pf}\\C_{ij}\tilde{n}_{j,t}\end{matrix}\right\|\leq C_{ij}\tilde{\pi}_{i,t} \tag{36}$$

The operation optimization of the integrated energy system is a typical multi-objective optimization problem under the diversified energy supply

model, involving several nonlinear, discrete, stochastic, and uncertain elements. Multi-constrained and multi-objective operation optimization models should be constructed to as closely represent the real state of system operation as feasible [23]. The findings of the multi-objective operation optimization model are not unique, in contrast to the integrated energy system's single objective operation optimization model, and numerous sets of possible solutions exist. These feasible options make up the Pareto optimum solution set.

The model is solved using the SOGA method by the energy system's operational plan. During the computation, the optimized Pareto solution set can be obtained by the SOGA algorithm, and the fuzzy genus function is used to select the best solution from the optimal solution set. The satisfaction of decision-makers to this objective optimization is reflected in the degree of membership, and the optimal solution is obtained by synthesizing the fuzzy membership of each objective function.

First, the dominance of the goal characteristic in the Pareto answer set is calculated using Equation (37).

$$u_i^k = \begin{cases} 1, & F_i = F_i^{\min} \\ \dfrac{F_i^{\max} - F_i}{F_i^{\max} - F_i^{\min}}, & F_i^{\min} \le F_i \le F_i^{\max} \\ 0, & F_i = F_i^{\max} \end{cases} \tag{37}$$

The calculation weight is set to equal weight. The calculation formula is as follows.

$$u^k = \frac{\sum_{i=1}^{N_{\text{obj}}} \lambda_i u_i^k}{\sum_{k=1}^{N_p} \sum_{i=1}^{N_{\text{obj}}} \lambda_i u_i^k} \tag{38}$$

If all ability and capability of strength storage gear in the IEGES gadget are listed as optimization variables of the genetic algorithm, the iterative technique to acquire the ideal answer through cross-variation will lead to sluggish convergence and a lengthy optimization process. Reducing the quantity of optimization variables will efficiently enhance the operation velocity of the mannequin and make the goal characteristic optimized by using a genetic algorithm to converge faster. As proven in Figure 3, via the evaluation of gadget operation strategy, it can be considered that fuel boilers and electrically powered chillers are auxiliary power furnish gear of IEGES system, gasoline turbines, waste warmness boilers, absorption chillers, and a number sorts of power storage function and furnish electricity in accordance to the operation

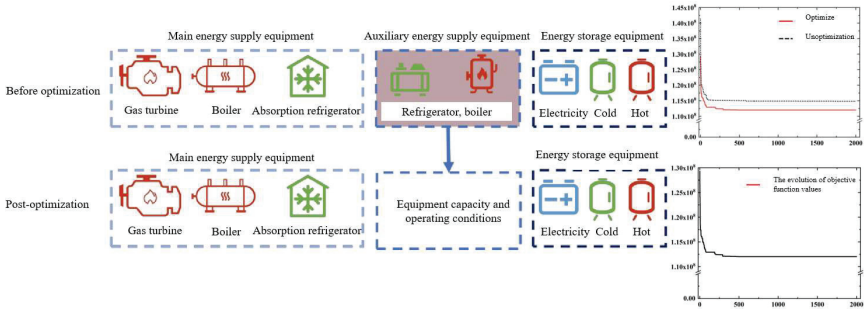

Figure 3 SOGA algorithm optimization and target optimization.

strategy, and gasoline boilers and electrically powered chillers supplement the inadequate heating and cooling [24]. Therefore, the operating conditions and required capacity of gas boilers and electric chillers are determined by the capacity and operating conditions of gas turbines, waste heat boilers, absorption chillers, and energy storage equipment. Therefore, in this study, the capacity of the gas boiler and electric refrigerator is removed from the optimization variable of the genetic algorithm, and the energy balance equation described in the previous section is adopted. The output of the gas boiler and electric refrigerator can be obtained at each time, and the maximum output is selected as the capacity of the equipment from the output of the whole year. The comparison of convergence before and after optimization of the number of variables in the SOGA algorithm is shown in Figure 3. After reducing the number of optimization variables, the convergence of optimization targets is accelerated.

In a genetic algorithm, parameters such as population size, crossover rate, variation rate, and iteration number will have a significant impact on the simulation process of the program. The essence of the genetic algorithm is to traverse various possible combinations of operators, and the population size and the number of iterations will affect the final simulation result from the possibility of traversal. If the population is too small, the program is easy to fall into the local optimal solution in the calculation process, if the population is too large. Although more population individuals can be generated, the amount of program calculation will increase exponentially and take a long time. Similarly, if the number of iterations is too small, the result may not converge; if the number of iterations is too large, it will increase the unnecessary calculation amount and take too long. The crossover rate refers to the probability that two individuals exchange some genes in the

genetic process and produce a new good variety. If the crossover rate is too small, more new individuals cannot be produced for selection, so the crossover rate should not be small. The rate of variation is the probability of changing an inherited gene (representing one bit of an individual's string of symbols). If the mutation rate is small, it is difficult to produce new genes, hindering the evolution of individuals, and the mutation rate is large. Then the randomness of population evolution is too large, and the iterative convergence may be poor. When the variation rate reaches 1, the genetic algorithm degenerates into a random algorithm. Parameter combination attempt after a long time, the population size of 30, the number of iterations is 600, cross rate is 0.8, the heritability of 0.3. Based on the above parameters can be long when considering the operation achieve better convergence operation result.

4 Stochastic Optimization of Energy Internet Considering Comprehensive Demand Response

4.1 Energy Internet Random Optimization Model

The model in this chapter is oriented towards the energy Internet environment, and the system contains multiple park-level energy hubs connected through regional-level transmission networks. The model aims to meet the energy consumption requirements of end users while complying with the operational constraints of the energy Internet by reasonably arranging the system operation mode and the implementation of demand response strategies [25]. From the perspective of the upper regional-level system scheduler, the model considers the random fluctuations of wind power output to optimize the expected operating costs of the system under all wind power scenarios, as shown in Equation (39). Among them, the system operating costs include demand response cost unit start-up and shutdown cost, coal-fired unit operation cost, gas well gas supply cost, wind abandonment, and load-cutting penalty.

$$\min \sum_{s} P_{R,s} \cdot \left\{ C_{DR}^{s} + \sum_{t} \left[\sum_{i \notin GU} \left(S_{G(l,i,t)}^{\mathrm{ele,s}} + S_{GD,i,t}^{\mathrm{ele,s}} \right) + \sum_{i \notin GU} F_{i,t}^{c}(P_{i,t}^{s}) \right. \right.$$
$$\left. \left. + \sum_{sp} C^{gas} W_{sp,t}^{s} + \sum_{w} \omega L_{wind,w,t}^{s} + \sum_{r} \sum_{\{*\}} a^{|*|} L_{demand,s}^{\{*\},s} \right] \right\} \tag{39}$$

The upper region level system provides energy input to the energy hub, and its operation needs to meet the corresponding constraints. For each wind power scenario, there are the following constraints on unit combination, power system, natural gas system, gas storage equipment, etc.

For traditional thermal power units, the unit combination mode is limited by constraints (40)–(51). Constraint (40) limits the output range of thermal power units. Constraints (41) and (42) limit the rate at which the unit can climb up/down, respectively. In this chapter, the quadratic cost function of coal-fired units is segmented into a linear form with constraints (43)–(45).

$$P_i^{\min} u_{i,t}^s \le P_{i,t}^s \le P_i^{\max} u_{i,t}^s \quad \forall i, \forall t, \forall s \tag{40}$$

$$P_{i,t}^s - P_{i,t-1}^s \le R_i^{Ul}[1 - u_{i,t}^s(1 - u_{i,t-1}^s)] + P_i^{\min} u_{i,t}^s (1 - u_{t,t-1}^s) \quad \forall i, \forall t, \forall s \tag{41}$$

$$P_{i,t-1}^s - P_{i,t}^s \le R_i^{D}[1 - u_{i,t-1}^s(1 - u_{i,t}^s)] + P_i^{\mathrm{mun}} u_{i,t-1}^s (1 - u_{i,t}^s) \quad \forall i, \forall t, \forall s \tag{42}$$

$$F_{t,t}^c(P_{t,t}^s) = \sum_{NP} cg_{t,t,p} \cdot P_{t,t,p}^s \quad \forall i, \forall t, \forall s \tag{43}$$

$$P_{t,t}^s = \sum_{NP} P_{t,t,f}^s \quad \forall i, \forall t, \forall p, \forall s \tag{44}$$

$$0 \le P_{i,t,p}^s \le P_{i,p}^{\max} \quad \forall i, \forall t, \forall p, \forall s \tag{45}$$

Constraints (46) and (47) respectively calculate the start-up and shutdown costs of coal-fired units, and (48) and (49) respectively calculate the start-up and shutdown gas consumption of gas units.

$$S_{GU,i,t}^{ele,s} = S_{UG,i}^{ele}[u_{i,t}^s(1 - u_{t,t-1}^s)] \quad \forall i \notin NGU, \forall t, \forall s \tag{46}$$

$$S_{GD,i,t}^{ele,s} = S_{DG,i}^{e/e}[u_{t,t-1}^s(1 - u_{i,t}^s)] \quad \forall i \notin NGU, \forall t, \forall s \tag{47}$$

$$S_{GU,i,t}^{gus,s} = S_{UG,i}^{gas}[u_{i,t}^s(1 - u_{i,t-1}^s)] \quad \forall i \in NGU, \forall t, \forall s \tag{48}$$

$$S_{GD,i,t}^{gas,s} = S_{DG,i}^{gas}[u_{i,t-1}^s(1 - u_{i,t}^s)] \quad \forall i \in NGU, \forall t, \forall s \tag{49}$$

$$(X_{i,t-1}^{\mathrm{on}} - T_i^{\mathrm{on}}) \cdot (u_{i,t-1}^s - u_{i,t}^s) \ge 0 \quad \forall i, \forall t, \forall s \tag{50}$$

$$(X_{i,t-1}^{\mathrm{off}} - T_i^{\mathrm{off}}) \cdot (u_{i,t}^s - u_{i,t-1}^s) \ge 0 \quad \forall i, \forall t, \forall s \tag{51}$$

Generally, DC power flow is used to analyze the regional power network. Equation (52) is the power balance constraint. Equation (53) uses the DC method to calculate the up flow of the transmission line h_j and uses Equation (54) to limit its maximum transmission capacity. Constraint (55) is the phase Angle constraint of nodes, and the equilibrium node must be set as the phase Angle reference node. Constraint (56) indicates that the wind could abandoned if necessary to ensure the safe operation of the system.

$$\sum_{i} T_{1,j,i} P_{i,l}^{s} + \sum_{hj} T_{2,j,hj} f_{hj,t}^{s} - \sum_{r} T_{6,j,r} E_{in,r,t}^{clc,s} + \sum_{w} T_{7,j,w} (P_{wind,w,j}^{s} - L_{wind,w,t}^{s}) = 0 \quad \forall j, \forall t, \forall s \tag{52}$$

$$f_{hj,t}^{s} = B_{hj} \cdot (\theta_{h,t}^{s} - \theta_{j,t}^{s}) \quad \forall hj, \forall t, \forall s \tag{53}$$

$$-f_{hj}^{\max} \le f_{hj,t}^{s} \le f_{hj}^{\max} \quad \forall hj, \forall t, \forall s \tag{54}$$

$$-\theta_{j}^{\max} \le \theta_{j,t}^{s} \le \theta_{j}^{\max} \quad \forall j, \forall t, \forall s \tag{55}$$

$$0 \le L_{wind,w,t}^{s} \le P_{wind,w,t}^{s} \quad \forall w, \forall t, \forall s \tag{56}$$

Natural gas system constraints:

$$W_{sp}^{\min} \le W_{sp,t}^{s} \le W_{sp}^{\max} \quad \forall sp, \forall t, \forall s \tag{57}$$

$$\pi_{m}^{\min} \le \pi_{m,t}^{s} \le \pi_{m}^{\max} \quad \forall m, \forall t, \forall s \tag{58}$$

$$\sum_{n \in GN_m} (g_{mn,t}^{ont,s} - g_{mn,t}^{in,s}) + \sum_{sp} T_{4,m,sp} W_{sp,t}^{s} + \sum_{q} T_{8,m,q} (G_{D,q,t}^{s} - G_{C,q,t}^{s}) - L_{m,t}^{s} = 0 \quad \forall m, \forall t, \forall s \tag{59}$$

$$L_{m,t}^{s} = \sum_{t} T_{s,m,t} (F_{i,t}^{gas,s} + S_{GU,i,t}^{gos,s} + S_{GD,i,t}^{gaas,s}) + \sum_{r} T_{9,m,r} \cdot \gamma E_{m,r.r.t}^{gas,s} \quad \forall m, \forall t, \forall s \tag{60}$$

Coupling constraints:

Because the thermal power unit has a large start-stop inertia, it can only perform output climbing in a short time, and its on/off state cannot be changed immediately. Therefore, each wind power scenario should have a completely consistent unit combination strategy [26]. Constraint (61) Limits the coupling

relationship of each scenario, that is, when making the plan, it is necessary to first establish the start-up and shutdown plan of thermal power units, and then adjust the decision values of other control variables (unit output, gas supply from gas Wells, status of gas storage equipment, wind abandonment, load cutting, demand response, etc.) according to the actual fluctuation of wind power.

$$u_{i,t}^{s} = u_{i,t}^{s'} \quad \forall i, \forall t, \forall s' \neq s \tag{61}$$

As the key coupling equipment, the gas unit connects the power and natural gas networks in the regional energy system and constitutes the coupling constraint between the energy networks. Constraint (62) represents the gas-electric conversion relationship in a gas unit.

$$P_{i,t}^{s} = \varphi_{NGU} F_{i,t}^{gas.s} \quad \forall i \in GU, \forall t, \forall s \tag{62}$$

4.2 Consider Demand Response Strategies for Energy Hubs

Figure 4 depicts the internal structure of a typical energy hub. The energy hub consists of three types of energy conversion equipment, namely a combined heat and power unit (CHP), an electric boiler (EB), and a heat storage unit (HS). CHP units take natural gas as an energy input from the upper region level system and convert it into electricity for use by end users and electric boilers. The heat generated by the CHP during power generation is transmitted to the end user or stored in the thermal storage unit: the electric boiler takes electrical energy from the transmission network and the CHP as energy input and converts it into thermal energy for the end user or storage in the thermal storage unit [27]. Heat storage units store energy from CHP and EB when there is an energy surplus and supply heat to users during peak heating periods. From the perspective of energy flow and mutual conversion,

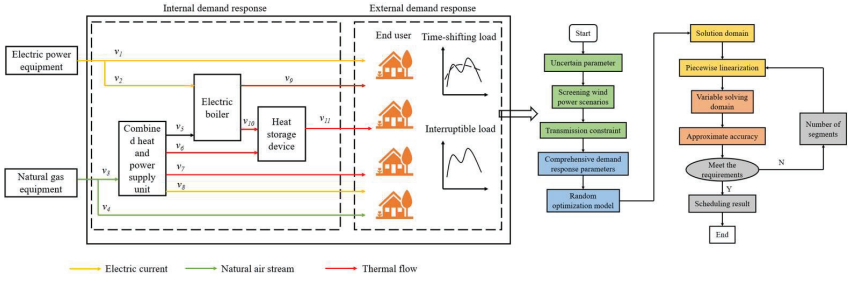

Figure 4 Illustration of the integrated demand response considering an energy hub.

the energy quality in the energy hub decreases step by step according to gas-electricity, which effectively realizes the cascade utilization of energy.

Based on the coupling relationship of energy flow above, the energy hub can be abstracted as a coupling unit with multiple energy inputs and outputs.

$$V_{in,r}^{s} = [E_{in,r,t}^{ele,s}, E_{in,r,t}^{gas.\mathrm{s.s}}, \Delta E_{r,t}^{s}, v_{1,r,t}^{s}, v_{2,r,t}^{s}, \ldots, v_{1,,r,t}^{s}]^{T} \quad \forall r, \forall t, \forall s \tag{63}$$

$$V_{out,t}^{s} = [E_{ous,r,t,}^{ele,s}, E_{out,r,t}^{gas,s}, E_{out,r,t}^{heat,s}, 0, \ldots, 0]^{T} \quad \forall r, \forall t, \forall s \tag{64}$$

According to Figure 4, there are complex correlations among energy flows, which are reflected in the following aspects. The first is the input/output energy flow constraint on the exit/entrance of the hub.

$$v_{1,r,t}^{s} + v_{2,r,t}^{s} = E_{in,r,t}^{ele,s} \quad \forall r, \forall t, \forall s \tag{65}$$

$$v_{3,r,t}^{s} + v_{4,r,t}^{s} = E_{in,r,t}^{gas,s} \quad \forall r, \forall t, \forall s \tag{66}$$

$$v_{1,r,t}^{s} + v_{8,r,t}^{s} = E_{oul,r,t}^{ele,s} \quad \forall r, \forall t, \forall s \tag{67}$$

$$v_{4,r,t}^{s} = E_{outr,r,t}^{gas,s} \quad \forall r, \forall t, \forall s \tag{68}$$

Time-shiftable load refers to the type of load that can be flexibly transferred from peak to valley according to the system guidance. Since this demand response is spontaneously completed by users guided by price or policy factors, it generally does not have a significant impact on user experience, and operators do not need to pay additional dispatch costs for this. Constraints (69)–(71) limit the time-shifting load of the three energy forms of electricity, gas, and heat. Constraints (69) and (70) respectively limit the maximum load that can be transferred in or out of the energy hub r during the t period. Constraint (71) indicates that in the whole dispatching cycle, the total amount of time-shifted load of the same type of energy remains unchanged after the demand response.

$$0 \leq R_{Sl,r,t}^{(*),s} \leq R_{Sl,r}^{(*),\max} \quad \forall r, \forall t, \forall s \tag{69}$$

$$0 \leq R_{SO,r,t}^{\{*\},s} \leq R_{SO,r}^{\{*\},\max} \quad \forall r, \forall t, \forall s \tag{70}$$

$$\sum_{t} R_{Sl,r,t}^{(*),s} = \sum_{t} R_{SO,r,t}^{\{*\},s} \quad \forall r, \forall t, \forall s \tag{71}$$

Interruptible load refers to the type of load that is actively interrupted according to the needs of the system during the peak operation of the system.

It is generally contracted in advance between the system operator and the end user to retain interruptible demand capacity for invocation. Equation (72) is the response cost of interruptible load, including the capacity cost generated by reserving interruptible capacity and the energy cost generated by actually invoking the interrupt. Formula (73) limits the interruptible load used in each scenario to the signed interruptible capacity range. Interruptible capacity is determined in advance in day-ahead scheduling and does not adjust to changes in wind and electricity scenarios.

$$C_{DR}^{s} = \sum_{r} \sum_{\{*\}} \left(\lambda^{\mathrm{CAP},\{*\}} \cdot R_{l,r}^{\{*\},\max} + \lambda^{IL,\{*\}} \cdot \sum_{t} R_{l,r,t}^{\{*\},s} \right) \quad \forall s \tag{72}$$

$$0 \leq R_{l,r,t}^{\{*\},s} \leq R_{l,r}^{\{*\},\max} \quad \forall r, \forall t, \forall s \tag{73}$$

4.3 Model Solving and Analysis

The overall process of the stochastic optimization algorithm for energy Internet proposed in this chapter is shown in Figure 4. Firstly, a stochastic optimization model considering energy network and comprehensive demand response is established, and then a continuous piecewise-linearization method is adopted to solve it.

In this section, the strength gadget containing 3EH and 17EH is tested, and the proposed mannequin and algorithm are verified. The small gadget in most cases analyzes the power conversion mode, gasoline storage equipment, complete demand response, and random fluctuations of wind power, whilst the massive gadget in the main checks the computational overall performance of the non-stop piecewise linearization algorithm. Load slicing and wind abandonment penalties are set at a thousand \$/MWh and 20 \$/MWh respectively. The potential and strength compensation charges for interruptible masses are set at 1 \$/MW and one hundred \$/MWh, respectively.

Figure 5 shows the composition of each energy input in the energy hub. Each hub obtains natural gas and electricity resources from the upper transmission system for internal conversion of the energy hub. In the energy flow input, natural gas resources account for the largest proportion, reaching 56.3%. This is because compared with traditional thermal power generation, obtaining natural gas directly from the natural gas network can avoid the loss in the power generation process, and the energy utilization efficiency is higher. The remaining energy input is power resources, of which thermal

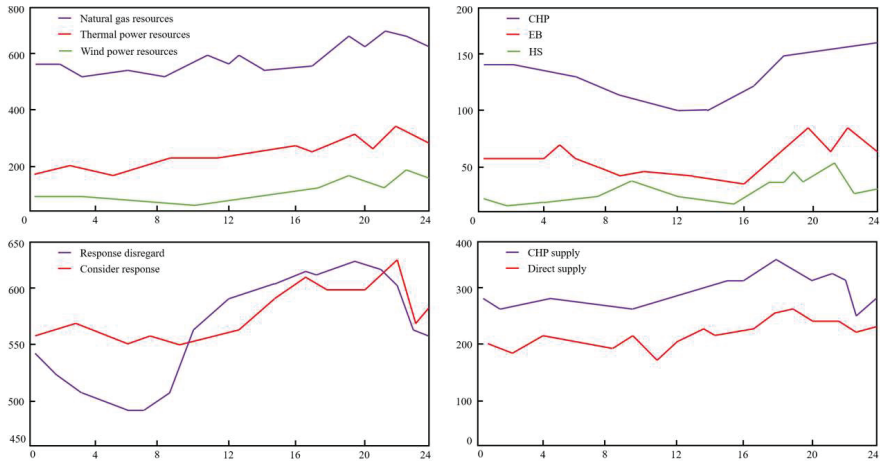

Figure 5 Energy system test results.

power and wind power resources account for 30.6% and 13.1% respectively. As you can see from the figure since the CHP has the highest energy conversion efficiency, most of the end user's thermal demand is provided by the CHP. Especially during the noon period (12 h∼16 h), all the heat energy is converted by the CHP equipment. At night, with the increase in users' heat demand, CHP heat production alone can no longer meet the requirement, and at this time, the hub has to call electric boilers and heat storage equipment to provide heat. However, even so, due to system congestion and insufficient construction capacity, there is still 263.56 MWh of heat demand that cannot be met, resulting in a lot of loads cutting losses. In the future, it is necessary to increase the investment in infrastructure and improve the system's energy supply capacity to better meet the needs of users. The end user's electricity needs can be met by the CHP burning natural gas or directly from the upper network. In contrast, direct access to electricity is more efficient because there is no energy conversion loss, and is the first choice for end-user power supply. Figure 5 shows how end-user power is supplied after the introduction of demand response. Under the function of internal demand response, EH can freely choose whether to use CHP to generate electricity or directly obtain electricity from the upper network. The energy hub can meet the energy demand of users by choosing a more economical and safe supply mode. At night (1 h∼6 h, 22 h∼24 h), the energy hub is more inclined to directly distribute the power from the upper layer to the user terminal due to the consideration of system congestion and conversion efficiency.

During daytime hours, the share of power generated by CHP increases due to certain congestion in the power system. Power supply mode is not fixed, the scheduling cycle cogeneration power share of 23.6% during the day, and night had fallen to 17.7%.

5 Conclusion

With the rapid growth of the domestic economy, people's living standards are increasingly rising, but it also leads to serious energy depletion and environmental pollution crisis. Considering demand response, this paper presents the optimal design and power metering of a power-gas interconnection energy system. In this paper, an optimization model of IEGES taking demand response into account is established. The energy conversion relationship and different energy flow directions of the electric-gas coupling equipment are described from three aspects: energy input, energy combination, and energy consumption. Taking demand response into account, the stochastic optimization of an electric-gas energy network is proposed. Specific conclusions are as follows.

1. This paper introduces a general demand response model on the power side, constructs a price-based demand response model, establishes an objective function considering power purchase cost, network loss cost, and wind and light abandonment cost, and proposes a decoupling cooperative scheduling optimization model of IEGES taking demand response into account. SOGA used to be used to clear up the model. After a lengthy time of parameter mixture attempts, the cutting-edge populace dimension is 30, a lot of iterations is 600, the crossover price is 0.8, and the heritability is 0.3. The above parameters can reap better convergence outcomes on the foundation of thinking about the operation time.
2. In this paper, a stochastic optimization method for energy Internet considering comprehensive demand-side response is proposed. The energy Internet can be represented as an interconnected comprehensive system with multiple energy hubs as the core, and energy starts from the upstream energy network and is finally transmitted and distributed to the end users in the energy hub. Based on this background, a comprehensive energy demand response model including external and internal demand response is constructed. Power supply mode is not fixed, the scheduling cycle cogeneration power share of 23.6% during the day, and night had fallen to 17.7%.

This paper mainly focuses on the operational level. But in fact, demand response can ease system congestion by flattening the load curve, delaying equipment maintenance and system investment. In the future, a comprehensive energy system joint planning model considering demand response can be established to make decisions on the location and capacity determination of multiple types of equipment in the energy network, and the rationality of the planning scheme can be measured by comprehensively considering random factors such as demand response uncertainty, equipment failure, and new energy fluctuations. Furthermore, based on multi-agent environment, a distributed planning method for multiple investment decision centers is studied to reduce the dependence among intelligent agents.

References

[1] Coltro L, Garcia E E C, Queiroz G C. Life cycle inventory for electric energy system in Brazil[J]. The International Journal of Life Cycle Assessment, 2003, 8: 290–296.

[2] Zimmermann T, Keil P, Hofmann M, et al. Review of system topologies for hybrid electrical energy storage systems[J]. Journal of Energy Storage, 2016, 8: 78–90.

[3] He Yufei, Wang Wei, Xiong Xiaofu et al. Pre-disaster cooperative scheduling strategy for emergency resources to improve the resiliency of power-gas interconnection energy system [J]. Automation of Electric Power Systems, 2019, 47(14): 21–32.

[4] Qiu Gefei, He Chao, Luo Zhao, et al. Fuzzy optimal scheduling of power-gas interconnection integrated energy system in industrial Park considering the uncertainty of source and load [J]. Electric power automation equipment, 2022, and (5): 8 to 14. DOI: 10.16081/j.page.202201015.

[5] Li Jinghua, Wang Zhibang, Jiang Juan. Optimization Planning of Electric-Gas Interconnection Transmission Network Considering Energy Supply Reliability [J]. Electric Power Automation Equipment/ Dianli Zidonghua Shebei, 2021, 41(9).

[6] Wei Zhenbo, Guo Yi, Wei Pingxi et al. Multi-objective extended planning model for integrated energy system of electric-gas interconnection based on IGDT [J]. High Voltage Technology, 2022, 48(02): 526–537. (in Chinese) DOI: 10.13336/j.1003-6520.hve.20201730.

[7] Elgerd O I, Fosha C E. Optimum megawatt-frequency control of multiarea electric energy systems[J]. IEEE transactions on power apparatus and systems, 1970 (4): 556–563.
[8] Vega A M, Santamaria F, Rivas E. Modeling for home electric energy management: A review[J]. Renewable and Sustainable Energy Reviews, 2015, 52: 948–959.
[9] Strasser T, Andren F, Kathan J, et al. A review of architectures and concepts for intelligence in future electric energy systems[J]. IEEE Transactions on Industrial Electronics, 2014, 62(4): 2424–2438.
[10] Tacker E C, Lee C C, Reddoch T W, et al. Optimal control of interconnected, electric energy systems – A new formulation[J]. Proceedings of the IEEE, 1972, 60(10): 1239–1241.
[11] Kamali S, Amraee T. Blackout prediction in interconnected electric energy systems considering generation re-dispatch and energy curtailment[J]. Applied Energy, 2017, 187: 50–61.
[12] Khan K R, Rahman M, Masrur H, et al. Electric energy exchanges in interconnected regional utilities: A case study for a growing power system[J]. International Journal of Electrical Power & Energy Systems, 2019, 107: 715–725.
[13] Zakeri B, Syri S. Electrical energy storage systems: A comparative life cycle cost analysis[J]. Renewable and sustainable energy reviews, 2015, 42: 569–596.
[14] Sansaniwal S K, Sharma V, Mathur J. Energy and exergy analyses of various typical solar energy applications: A comprehensive review[J]. Renewable and Sustainable Energy Reviews, 2018, 82: 1576–1601.
[15] Yu S, Zheng Y, Li L. A comprehensive evaluation of the development and utilization of China's regional renewable energy[J]. Energy Policy, 2019, 127: 73–86.
[16] Kyriakopoulos G L, Arabatzis G. Electrical energy storage systems in electricity generation: Energy policies, innovative technologies, and regulatory regimes[J]. Renewable and Sustainable Energy Reviews, 2016, 56: 1044–1067.
[17] Sezer N, Koç M. A comprehensive review on the state-of-the-art of piezoelectric energy harvesting[J]. Nano energy, 2021, 80: 105567.
[18] Meng Q W, Guan Q S, Jia N, et al. An improved sequential energy flow analysis method based on multiple balance nodes in gas-electricity interconnection systems[J]. IEEE Access, 2019, 7: 95487–95495.

[19] Lai C S, Jia Y, Lai L L, et al. A comprehensive review on large-scale photovoltaic system with applications of electrical energy storage[J]. Renewable and Sustainable Energy Reviews, 2017, 78: 439–451.
[20] Sidhu A S, Pollitt M G, Anaya K L. A social cost benefit analysis of grid-scale electrical energy storage projects: A case study[J]. Applied energy, 2018, 212: 881–894.
[21] Zhang Y, Liu W, Shi Q, et al. Resilience assessment of multi-decision complex energy interconnection system[J]. International Journal of Electrical Power & Energy Systems, 2022, 137: 107809.
[22] Luo X, Wang J, Dooner M, et al. Overview of current development in electrical energy storage technologies and the application potential in power system operation[J]. Applied energy, 2015, 137: 511–536.
[23] Cebulla F, Naegler T, Pohl M. Electrical energy storage in highly renewable European energy systems: Capacity requirements, spatial distribution, and storage dispatch[J]. Journal of Energy Storage, 2017, 14: 211–223.
[24] Mamade A, Loureiro D, Alegre H, et al. A comprehensive and well tested energy balance for water supply systems[J]. Urban Water Journal, 2017, 14(8): 853–861.
[25] Gissey G C, Dodds P E, Radcliffe J. Market and regulatory barriers to electrical energy storage innovation[J]. Renewable and Sustainable Energy Reviews, 2018, 82: 781–790.
[26] Kebede A A, Kalogiannis T, Van Mierlo J, et al. A comprehensive review of stationary energy storage devices for large scale renewable energy sources grid integration[J]. Renewable and Sustainable Energy Reviews, 2022, 159: 112213.
[27] Battistelli C, Baringo L, Conejo A J. Optimal energy management of small electric energy systems including V2G facilities and renewable energy sources[J]. Electric Power Systems Research, 2012, 92: 50–59.

Biographies

QianQian Cai Graduated from Huazhong University of Science and Technology with a master's degree. After graduation, worked at the Measurement Center of Guangdong Power Grid Co., Ltd., mainly researching the operation analysis, architecture, and application optimization of measurement automation systems. I am currently an in-service engineer.

Xiao Jiang Graduated from South China Normal University with a master's degree in software engineering. After graduation, I worked at the Measurement Center of Guangdong Power Grid Co., Ltd. My main research direction is cryptography and information security. The current professional title is Intermediate Engineer.

ZheHeng Liang Graduated from Beijing Normal University Zhuhai Branch with a bachelor's degree in Information Management and Information Systems. After graduation, I worked at the Information Center of Guangdong Power Grid Co., Ltd., mainly researching digitalization. The current professional title is Senior Engineer.

ShiMeng Du Graduated from North China Electric Power University with a master's degree, majoring in detection technology and automation devices. After graduation, I worked at Yunfu Power Supply Bureau of Guangdong Power Grid Co., Ltd., mainly in the fields of measurement automation application and electric energy data management. The current professional title is Engineer.

ShiFeng Jiang Graduated from Sun Yat sen University with a bachelor's degree, and later employed at Guangzhou Luoli Energy Technology Co., Ltd., mainly researching the field of electricity. The current professional title is Senior Engineer.